

Axisymmetric deformations of neutron stars and gravitational-wave astronomy

Guilherme Raposo^{1,*} and Paolo Pani^{1,†}

¹*Dipartimento di Fisica, “Sapienza” Università di Roma & Sezione INFN Roma1, Piazzale Aldo Moro 5, 00185, Roma, Italy*

Einstein’s theory of general relativity predicts that the only stationary configuration of an isolated black hole is the Kerr spacetime, which has a unique multipolar structure and a spherical shape when nonspinning. This is in striking contrast to the case of other self-gravitating objects, which instead can in principle have arbitrary deformations even in the static case. Here we develop a general perturbative framework to construct stationary stars with small axisymmetric deformations, and study explicitly compact stars with an intrinsic quadrupole moment. The latter can be sustained, for instance, by crust stresses or strong magnetic fields. While our framework is general, we focus on quadrupolar deformations of neutron stars induced by an anisotropic crust, which continuously connect to spherical neutron stars in the isotropic limit. Deformed neutron stars might provide a more accurate description for isolated and binary compact objects, and can be used to improve constraints on the neutron-star equation of state through gravitational-wave detections and through the observation of low-mass X-ray binaries. We argue that, for values of the dimensionless intrinsic quadrupole moment of few percent or higher (which can be sustained by an elastic crust with ordinary parameters), the effect of the deformation is stronger than that of tidal interactions in coalescing neutron-star binaries, and might also significantly affect the electromagnetic signal from accreting neutron stars. Current observational bounds on the post-Newtonian coefficients in the gravitational waveform signal from GW170817 do not exclude that the neutron stars in the binary had some significant intrinsic deformation.

I. INTRODUCTION

Neutron stars (NSs) harbor the highest densities, the strongest magnetic fields, the highest binding energy per nucleon, and the strongest spacetime curvatures in the universe. Provided their interior and spacetime can be accurately modeled using nuclear physics and general relativity, NSs are unique probes of all fundamental interactions and ideal laboratories to test foundational physics and high-energy astrophysics [1].

However, at variance with black holes, NSs are not simple objects. Within Einstein’s theory of general relativity, the black-hole uniqueness theorems imply that the ultimate stationary outcome of the gravitational collapse must be a Kerr black hole [2, 3]. The latter has an infinite number of multipole moments [4] which are anyway uniquely determined in terms of its mass and angular momentum [5]. When nonspinning, any isolated black hole in the universe must be spherically symmetric and described by the Schwarzschild spacetime.

This remarkable simplicity does not hold true for other self-gravitating objects, in particular for NSs. There is no compelling reason preventing NSs to be arbitrarily deformed away from spherical symmetry, even when nonspinning. In fact, one might even argue the opposite, namely that spherical symmetry is a mere idealization and that all astrophysical formation processes are intrinsically *asymmetric*, e.g., due to magnetic fields, environmental effects, crust shears, elasticity, turbulence, convective instabilities, collimated neutrino fluxes, gravitational-wave (GW) emission, kicks, deformations

of the progenitor proto-NS, etc. It is therefore natural to expect that a newly-born NS might be deformed to some degree and that it can reach a stationary, *axisymmetric* (but not necessarily spherical) configuration through GW emission [6] over long time scales.

In this paper we are not interested to model the complex physical mechanisms (e.g., core-collapse supernovae [7, 8] or a compact-binary coalescence [9–11]) that may lead to the formation of a highly deformed stars, but rather we wish to understand whether realistic matter can sustain *stationary* stars which deviate from spherical symmetry. While it is possible that the processes mentioned above lead to large deviations from sphericity, we shall work in a perturbative regime and treat these deviations as small perturbations around a spherical star. This approximation is also consistent with the fact that – to the best of our knowledge – these deformations have been so far neglected when modelling stationary sources, e.g. old NS in low-mass X-ray binaries or in coalescing binaries.

Non-axisymmetric deformations have been intensively studied as a source of quasi-monochromatic GWs from isolated spinning NSs [12–14]. Strong constraints exist on departures from axisymmetry, typically measured by the ellipticity of a NS [12, 15–17]. Additionally, axisymmetric deformations have also been studied in the past, especially in the context of magnetized [18–23] or spinning [24, 25] stars. However, in the absence of magnetic fields or rotation, deformations can only be supported by the elastic properties of the material. The elastic properties of NSs are under active scrutiny, both in the stellar core [26–28] and in the crust (see, e.g., Ref. [29] for a review on the topic). Although axisymmetric deforma-

* guilherme.raposo@roma1.infn.it

† paolo.pani@uniroma1.it

tions do not destabilize the star through GW emission¹, they might give rise to important effects in isolated and binary NSs. The scope of this work is to discuss this scenario. Unless otherwise stated, we use $G = c = 1$ units henceforth.

Executive Summary

For the reader's convenience, here we summarize the main results of our work in nontechnical terms, the technical computation is presented in Sec. II. We have developed a general-relativistic, perturbative framework to construct equilibrium configurations of self-gravitating bodies with small (but otherwise generic) axisymmetric deformations away from spherical symmetry. Our approach is based on a framework recently developed for vacuum spacetimes [31] and extends the latter to the case of matter fields, in particular perfect fluids, which provide an accurate description of the interior of cold NSs. We consider a spherical-harmonic decomposition of the spacetime and of the stress-energy tensor, and solve for Einstein's field equations in the interior of the star perturbatively in the deformations. The numerical solution in the stellar interior is then matched to the analytical solution known in the exterior [31], using appropriate boundary conditions (cf. Sec. II A 3). Spherical NSs deformed by an intrinsic small angular momentum (constructed in the seminal papers by Hartle and Thorne [24, 25]) are a particular case of our general framework, which can be straightforwardly extended to arbitrary intrinsic multipole moments, to any perturbative order, and to different matter content. The framework is also similar to the linear perturbations of NSs due to tidal effects [32], although in our case there is no external source term such as a tidal field. For this reason we refer to the deformations as *intrinsic* multipole moments, as opposed to the spin-induced or tidally-induced ones. In the following we shall focus on the most interesting case of *quadrupolar* deformations, being $\bar{Q} = Q/M^3$ the dimensionless quadrupole moment of a star with mass M .

In the absence of source terms (e.g. tidal fields, angular momentum, magnetic fields, shears, etc), the metric that describes a self-gravitating, perfect fluid with a quadrupolar deformation is discontinuous across the surface of the object. This shows that a (single) perfect-fluid star does not support deviations away from spherical symmetry in the static case [33]. However, here we show how an *anisotropic* crust can support relatively large quadrupolar deformations. The standard equation

of state (EoS) of a NS includes also the relatively low-density region of the crust [1, 29], but typically assuming a perfect fluid for the latter, and therefore neglecting possible anisotropies. In reality the crust of a NS is crystallized, i.e. atomic nuclei form a lattice [29, 34, 35] whose elasticity can support asymmetric distributions [30]. The (micro)physical processes of the crust are complex and model dependent. In an attempt to build a more general and less model-dependent configuration, we model the NS crust with a thin shell made of an anisotropic fluid and then match its properties with those of a more realistic crust model. In the deformed case the discontinuity of the metric across the stellar radius, together with the junction conditions at the surface [36, 37], dictate the properties of the thin shell.

We have thus constructed explicitly a two-parameter family of NS equilibrium configurations characterized – for each value of the central density ρ_c – by an intrinsic quadrupole moment Q , which is proportional to the anisotropy of the thin-shell crust. It is straightforward to add angular momentum J perturbatively in our framework, so this family of solutions can be extended to a three-parameter model. For each value of (ρ_c, J, Q) , we can compute the other properties of the star, including the mass M and radius R . We stress that these solutions can be asymmetric even when nonrotating; for this reason we refer to them as *deformed NSs*. An illustrative diagram of these solutions is presented in Fig. 1.

The junction conditions imply that the crust is made of an anisotropic fluid, whose surface energy density can be written in general as

$$\sigma(\theta) = \sigma_0 + \sigma_2 \bar{Q} P_2(\cos \theta), \quad (1)$$

where the free parameter $\sigma_0 \sim M_{\text{crust}}/(4\pi R^2)$ is the surface density of the crust in the spherical configuration, σ_2 is the (normalized) amplitude of the axisymmetric perturbation to the surface density, and $P_\ell(\cos \theta)$ is the Legendre polynomial ($\ell = 0, 1, 2, \dots$). The anisotropy of the fluid on the thin shell can be measured by the difference

$$\Delta\gamma \equiv \gamma_\theta - \gamma_\phi = \bar{Q} \frac{3 \sin^2 \theta}{8\pi R^2 \sqrt{1 - 2M/R}} [[\xi]], \quad (2)$$

between the surface pressure γ along the two angular directions, where $[[\xi]]$ is the jump of the fluid displacement at the radius (see Sec. II A 3 for details). Note that both the monopolar and quadrupolar components of the pressure are anisotropic.

In Fig. 2 we show the surface energy density $\bar{Q}\sigma_2$ (see Eq. (1)) and the surface pressure anisotropy $\Delta\gamma$ (see Eq. (2)) at the equator as a function of the NS compactness for some relevant EoS. We normalize both quantities by the quadrupole value $|\bar{Q}| = 0.1$, and by typical reference values, $\sigma_0 \sim 10^{18} \text{ g cm}^{-2}$ and $\gamma_0 \sim 10^{17} \text{ g cm}^{-2}$, respectively, roughly corresponding to a crust containing 1% of the total NS mass [29]. In particular, the values of the anisotropic pressure shown in Fig. 2 are compatible with the maximum allowed by elasticity of the crust,

¹ GW emission from axisymmetric NSs can occur only if the stellar angular momentum is misaligned with the axis of symmetry, leading to precession. We focus here on stationary configurations, for which the angular momentum (if present) coincides with the axis of symmetry.

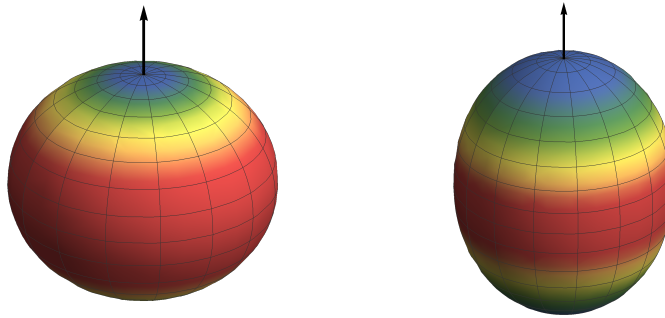


FIG. 1. **Deformed NSs.** Illustrative embedding diagrams of a deformed NS. The arrow is the angular momentum vector and (if present) coincides with the axis of symmetry. The colors are weighted to represent the current multipole moment. In this example the body on the left is oblate due to a negative intrinsic quadrupole moment which adds to the spin-induced term (the latter contributes to make the star oblate), whereas the body on the right is prolate because the effect of a positive intrinsic quadrupole moment is stronger than the spin contribution.

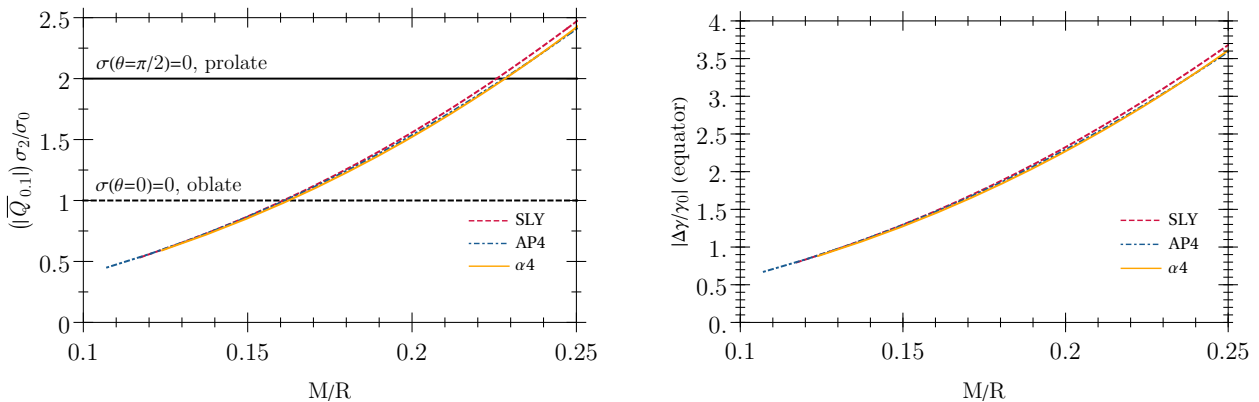


FIG. 2. **Properties of the crust thin-shell.** *Left panel:* quadrupolar surface density $\bar{Q}\sigma_2$ obtained with different tabulated EoS. This quantity is normalized by a quadrupole value $|\bar{Q}| = 0.1$ and by a typical reference value for the spherical surface density of the shell σ_0 , corresponding to 1% of the NS mass. Due to the quadrupolar deformation of the star, the density can be negative depending on the ratio between the magnitude of the quadrupolar density deformation and the spherical shell density. For prolate (oblate) configurations, the minimum value of the density occurs at the equator (poles) and the limit of zero density is represented by the horizontal solid (dashed) black line. When the ratio is below the black line, the surface density is positive everywhere, whereas it can be negative for values above the curve. *Right panel:* surface anisotropy $\Delta\gamma \equiv \gamma_\theta - \gamma_\phi$ at the equator, normalized by $\bar{Q} = 0.1$ and by the pressure of the spherical shell, γ_0 , corresponding to a crust with 1% of the NS mass. The quadrupolar deformation of the star induces anisotropy in the surface pressure of the star between the two angular directions. The relative magnitude is compatible with the maximum one allowed by elastic shears [30]. Note that both σ_2 and $\Delta\gamma$ grow monotonically with the compactness of the star and are almost independent of the EoS.

$\Delta\gamma/\gamma_0 \sim (0.005 - 0.04)Z^{4/3}$, where $Z \gtrsim 26$ is the atomic number of the ions in the crust (mostly iron in the outer crust [29]) and the prefactor depends on the type and direction of elastic deformations of the lattice [30]. The main result that can be inferred from Fig. 2 is the fact that realistic values of the crust properties can sustain an intrinsic quadrupole as high as $\bar{Q} = \mathcal{O}(0.1)$, with more conservative values being $\bar{Q} = \mathcal{O}(0.01)$. We shall discuss the phenomenological implications of this intrinsic quadrupole in Sec. III.

The rest of this paper is organized as follows. In the

Sec. II we present the details of the technique used to construct deformed NSs, discussing the background configuration in Sec. II A. A discussion on the energy conditions is presented in Sec. II B, whereas stability of the equilibrium configurations is discussed in Sec. II C. Finally, phenomenological effects of intrinsic deformations on the GW phenomenology are presented in Sec. III and discussed on Sec. IV.

II. AXISYMMETRIC DEFORMATIONS OF NSS: THIN-SHELL CRUST

In this section we present the technical computation to construct NSs with perturbative deformations away from spherical symmetry.

A. Equilibrium configurations

1. Formalism

Our technique is an extension of the perturbative, general-relativistic framework recently developed to study generic axisymmetric departures from spherical symmetry in vacuum spacetimes [31]. We first provide the general framework for an arbitrary number of independent multipolar deformations, and then specialize it to the case in which the only nonvanishing deformations are due to the mass quadrupole moment (and, possibly,

to the spin).

We consider a deformed metric of the form

$$g_{\mu\nu} = g_{\mu\nu}^{(0)} + \sum_{n=1}^{\infty} \epsilon^n h_{\mu\nu}^{(n)}, \quad (3)$$

where $g_{\mu\nu}^{(0)} = \text{diag} \{-e^{\nu(r)}, 1/(1-2m(r)/r), r^2, r^2 \sin^2 \theta\}$ is the background metric which describes the spherically-symmetric star and can be obtained by solving for the Tolman-Oppenheimer-Volkoff equations [6], ϵ is a small book-keeping parameter, and $h_{\mu\nu}^{(n)}$ is the deformation entering at order $\mathcal{O}(\epsilon^n)$. When only the mass quadrupole Q (and, possibly, the angular momentum J) are present at the leading order, the physical expansion parameters are the dimensionless quantities $\epsilon Q/M^3$ and $\epsilon J/M^2 \equiv \epsilon \chi$, which are independent from one another.

Stationary and axisymmetric deformations can be expanded in a complete basis of Legendre polynomials:

$$h_{\mu\nu}^{(n)} = \sum_{\ell} \begin{pmatrix} g_{00}^{(0)} H_0^{n\ell} P_{\ell} & 0 & 0 & h_0^{n\ell} P'_{\ell} \\ 0 & g_{rr}^{(0)} H_2^{n\ell} P_{\ell} & 0 & 0 \\ 0 & 0 & r^2 K^{n\ell} P_{\ell} & 0 \\ h_0^{n\ell} P'_{\ell} & 0 & 0 & r^2 \sin^2 \theta K^{n\ell} P_{\ell} \end{pmatrix}, \quad (4)$$

with $P_{\ell} = P_{\ell}(\cos \theta)$ and $P'_{\ell} = \frac{dP_{\ell}(\cos \theta)}{d \cos \theta}$. The parameter ℓ is related to the multipole moment sourced at each given order n of the perturbative scheme. We separate the perturbations in two sets, according to how they transform under parity. The odd (or axial) sector contains only the radial function $h_0^{n\ell}(r)$, which is associated to the *current* multipole moments, S_{ℓ} . The even (or polar) sector contains the radial functions $H_0^{n\ell}(r)$, $H_2^{n\ell}(r)$, and $K^{n\ell}(r)$, which are associated to the *mass* multipole moments, M_{ℓ} . Note that we defined the mass quadrupole moment as Q ; a more standard and general nomenclature is $Q \equiv M_2$ [4, 5].

We consider Einstein's equations coupled to a perfect fluid that describes the interior of the star. The fluid's stress-energy tensor reads

$$T^{\mu\nu} = (P + \rho)u^{\mu}u^{\nu} + P g^{\mu\nu}, \quad (5)$$

where

$$P = P^{(0)}(r) + \sum_{n=1}^{\infty} \sum_{\ell} \epsilon^n \delta P^{n\ell}(r) P_{\ell} \cos(\theta), \quad (6)$$

$$\rho = \rho^{(0)}(r) + \sum_{n=1}^{\infty} \sum_{\ell} \epsilon^n \delta \rho^{n\ell}(r) P_{\ell} \cos(\theta), \quad (7)$$

are the pressure and the energy density of the fluid, respectively, the background values of which are denoted by

$P^{(0)}(r)$ and $\rho^{(0)}(r)$. The functions $\delta P^{n\ell}(r)$ and $\delta \rho^{n\ell}(r)$ are polar quantities. The four-velocity of a fluid element reads

$$u^{\mu} = \frac{1}{\sqrt{-g_{tt} - 2\epsilon \Omega g_{t\phi} - g_{\phi\phi} \epsilon^2 \Omega^2}} \{1, 0, 0, \epsilon \Omega\}, \quad (8)$$

where Ω is the fluid angular velocity and the normalization constant ensures that $u^2 = -1$.

By inserting the above decomposition for the metric and the fluid variables into Einstein's equations, $G_{\mu\nu} = 8\pi T_{\mu\nu}$, and separating the angular dependence by using the orthogonality of the Legendre polynomials [31, 38], we obtain a set of ordinary differential equations for the deformation functions $h_{\mu\nu}^{(n)}(r)$, $\delta P^{(n)}(r)$, and $\delta \rho^{(n)}(r)$. The system is closed by assuming a barotropic EoS, $P = P(\rho)$.

In the exterior, the solution to the system can be found analytically at any given order and it depends on an arbitrary number of (mass and current) multipole moments [31]. The explicit values of the multipole moments can be obtained by matching the external solution to the internal one at the radius R of the star, defined by $P^{(0)}(r = R) = 0$ at the leading order. The internal solution is obtained numerically using a Runge-Kutta 4th order scheme with adaptive meshes [39].

The couplings between multipoles follow the standard

addition rules for angular momenta in quantum mechanics, so that if two modes with ℓ_1 and $\ell_2 > \ell_1$ are present at a given order in ϵ , to the next order they will source multipole moments with ℓ such that $\ell_2 - \ell_1 \leq \ell \leq \ell_2 + \ell_1$, provided some terms are not forbidden by parity and equatorial-symmetry selection rules [31]. In the specific case of deformations sourced by J and Q , only the $\ell = 1$ axial deformation and the $\ell = 2$ polar deformation are respectively present to $\mathcal{O}(\epsilon)$. Therefore, all induced multipole moments of this family of solutions can be written as a combination of terms sourced by the spin and by the quadrupole; to the leading order:

$$\bar{M}_\ell = \sum_{p=0}^{\ell/2} \alpha_p \chi^{\ell-2p} \bar{Q}^p, \quad \text{even } \ell \geq 4,$$

$$\bar{S}_\ell = \sum_{p=0}^{(\ell-1)/2} \beta_p \chi^{\ell-2p} \bar{Q}^p, \quad \text{odd } \ell \geq 3,$$

whereas $M_\ell = 0$ and $S_\ell = 0$ for odd ℓ and even ℓ , respectively. In the above equation, $\bar{M}_\ell = M_\ell/M^{\ell+1}$ and $\bar{S}_\ell = S_\ell/M^{\ell+1}$ are the normalized multipole moments of degree ℓ . The prefactors α_p and β_p depend on the central density and on the EoS and have to be computed numerically.

The solution can be computed to any given order using the set of rules discussed above. Nonetheless, to linear order in the perturbation framework the solution is very simple since it is not affected by the nonlinearities of the field equations.

2. Explicit external solution to leading order

In the exterior of the object the solution can be found analytically [31]. To the leading order it reads

$$g_{tt} = - \left(1 - \frac{2M}{r}\right) - \frac{5Q (2M (2M^3 + 4M^2r - 9Mr^2 + 3r^3) + 3r^2(r - 2M)^2 \log(1 - \frac{2M}{r}))}{8(M^5 r^2)} P_2, \quad (9)$$

$$g_{rr} = \left(1 - \frac{2M}{r}\right)^{-1} - \frac{5Q (2M (2M^3 + 4M^2r - 9Mr^2 + 3r^3) + 3r^2(r - 2M)^2 \log(1 - \frac{2M}{r}))}{8M^5(r - 2M)^2} P_2, \quad (10)$$

$$g_{\theta\theta} = r^2 - \frac{5Qr (-4M^3 + (3r^3 - 6M^2r) \log(1 - \frac{2M}{r}) + 6M^2r + 6Mr^2)}{8M^5} P_2, \quad (11)$$

$$g_{\phi\phi} = g_{\theta\theta} \sin^2 \theta, \quad (12)$$

$$g_{t\phi} = - \frac{2J \sin^2 \theta}{r}. \quad (13)$$

3. Thin-shell crust and junction conditions

We can solve numerically the equations for the deformation in the interior of the star and match them with the above analytical solution in the exterior using appropriate junction conditions [36, 37, 40, 41].

The first junction condition imposes continuity of the induced metric η_{ab} across the thin shell,

$$[[\eta_{ab}]] = 0, \quad (14)$$

where $[[X]] := X_{\text{out}} - X_{\text{in}}$ denotes a jump of a generic quantity X across the radius of the thin shell. To zeroth order in the deformations the first junction condition implies that

$$e^{\nu(R)} = 1 - 2M/R, \quad (15)$$

which is the usual continuity of time-time component of the metric, and can be imposed with a rescaling of the time coordinate in the interior of the star. To linear order this condition relates the jump of the metric functions

with the quadrupole of the NS,

$$[[H_0^{1\ell}]] = - \left[\left[\frac{f'}{f} \xi_2 \right] \right], \quad (16)$$

$$[[K^{1\ell}]] = - \frac{2}{R} [[\xi_2]], \quad (17)$$

where $f_{\text{out}} = 1 - 2M/r$, $f_{\text{in}} = e^\nu$, and $\xi := \xi_2 P_2(\theta)$ is the displacement of the thin shell.

The second junction condition relates the jump of the extrinsic curvature K_{ab} with the stress-energy tensor,

$$S_{ab} = \frac{1}{8\pi} ([[K_{ab}]] - \eta_{ab} [[K]]), \quad (18)$$

with $K = \eta_{ab} K^{ab}$. The surface energy density σ of the thin shell can be obtained as the eigenvalue of the stress energy tensor, namely

$$S_b^a u^b = -\sigma u^a. \quad (19)$$

The surface energy density can be written in general as in Eq. (1), where σ_0 is the surface density of the thin

shell in the spherically-symmetric configuration, whereas σ_2 is the amplitude of the axisymmetric perturbation to the surface density. By solving Eq. (19) we find the expressions for the surface density components in terms of the jump of metric functions. The zeroth order spherical case is particularly simple,

$$\sigma_0 = -\frac{1}{4\pi R} \left[\left[\left(g_{rr}^{(0)} \right)^{-1/2} \right] \right]. \quad (20)$$

Obviously, in the spherical-symmetric case the continuity of the mass function implies the absence of any shell of matter. Conversely, assuming the existence of a thin shell with mass $M_{\text{crust}} = \delta M := M - m(R)$ implies $[[g_{rr}^{(0)}]] \neq 0$ and the presence of a surface energy density given by Eq. (20). For small thin-shell masses Eq. (20) becomes

$$\sigma_0 = \frac{1}{4\pi R^2} \frac{\delta M}{\sqrt{1 - 2M/R}} + \mathcal{O}(\delta M^2), \quad (21)$$

which reduces to the Newtonian case $\sigma_0 = \delta M / (4\pi R^2)$ when $M/R \ll 1$.

By using the projection tensor $q_{ab} := \eta_{ab} + u_a u_b$, we can define the projected stress-energy tensor of the thin shell,

$$\gamma_{ab} = S^{cd} q_{ac} q_{bd}. \quad (22)$$

Again, the spherical case is particularly simple and it reduces to the stress-energy tensor of a perfect fluid,

$$\gamma_{ab} = \gamma_0 q_{ab}, \quad (23)$$

where γ_0 is the surface pressure of the shell. Comparing

$$\sigma_2 = \frac{1}{8\pi R} \left(\left[\left[\sqrt{1 - 2M/R} H_2 \right] \right] - \left[\left[\frac{4 + 6M/R}{R\sqrt{1 - 2M/R}} \xi_2 \right] \right] - \left[\left[R\sqrt{1 - 2M/R} K' \right] \right] \right). \quad (27)$$

A similar (albeit more involved) relation can be derived for the quantity $\Delta\gamma$ defined in Eq. (2). This anisotropy $\Delta\gamma$ is required to support the quadrupolar deformation. When the surface pressures along the two angular directions on the shell are identical, the boundary conditions described above imply that the quadrupole moment must vanish.

4. Examples of deformed NS configurations

To summarize, the metric and fluid variables obtained numerically in the interior of the object are then matched to the external solution through the above junction conditions. The numerical solutions form a 3-parameter family, which depends on the central density ρ_c , the angular momentum J (aligned with the symmetry axis, see

Eq. (22) with Eq. (23) yields

$$\gamma_0 = \frac{1}{8\pi R} \left[\left[\frac{1 + \frac{R}{2} \frac{f'}{f}}{\sqrt{g_{rr}^{(0)}}} \right] \right], \quad (24)$$

which for small thin-shell masses can be reduced to

$$\gamma_0 \sim \frac{M}{8\pi R^3} \frac{\delta M}{(1 - 2M/R)^{3/2}} + \mathcal{O}(\delta M^2). \quad (25)$$

To allow for quadrupolar deformations we will consider an anisotropic fluid for the matter of the thin shell, whose stress-energy tensor reads

$$\gamma_{ab} = \gamma^\theta k_a k_b + \gamma^\phi \chi_a \chi_b, \quad (26)$$

where k_a and χ_a are two normal vectors tangent to the thin shell, orthogonal to the fluid velocity u_a and among themselves, i.e. $\chi_a k^a = k_a u^a = \chi_a u^a = 0$, $k_a k^a = 1 = \chi_a \chi^a$. The latter five conditions do not specify the two vectors completely. There is one remaining degree of freedom which is related to the orientation of the two vectors with respect to the coordinate axis. One can fix this freedom by choosing to align k_a with the θ -axis and χ_a with the ϕ -axis. With this choice γ^θ and γ^ϕ are the components of the surface pressure measured along the θ and ϕ directions, respectively. To calculate the pressure components it is useful to decompose each of them as $\gamma^i = \gamma_0^i + \gamma_2^i P_2(\theta)$, and solve Eqs. (22) and (26) for the four independent pressure functions.

For example, the quadrupolar component of the surface energy density reads

Fig. 1) and the mass quadrupole moment $Q \equiv M_2$.

As a reference, in Table I we provide some relevant quantities of the equilibrium configurations obtained with this procedure and assuming the AP4 EoS. A representative example of the fluid and metric variables in the interior of a deformed NS is shown in Fig. 3.

B. Energy conditions

Due to the broken spherical symmetry of the system, there are values of the parameter space for which the density might be negative, i.e. when $\bar{Q}\sigma_2 P_2(\theta) < -\sigma_0$ (see Eq. (1)). However, as shown in Fig. 2, the surface density is always positive for a NS with $|Q| \lesssim 0.1$ and compactness $M/R \lesssim 0.15$. For the same range of quadrupole values, prolate stars have positive density for realistic

ρ_c [10^{15} g/cm 3]	Ω/Ω_K	$\bar{Q}/10^{-2}$	$m(R)$ [M_\odot]	R [km]	\bar{I}	$\bar{Q}\sigma_2/\sigma_0$	$ \Delta\gamma/\gamma_0 ^{\text{equator}}$	ν_ϕ^{ISCO} [kHz]	ν_θ^{ISCO} [kHz]
1.540	0	0	2.00	11.0	6.18	0	0	1.10	1.10
0.985	0	0	1.40	11.4	11.1	0	0	1.57	1.57
0.875	0	0	1.20	11.5	14.3	0	0	1.84	1.84
1.540	5%	0	2.00	11.0	6.18	0	0	1.13	1.13
0.985	5%	0	1.40	11.4	11.1	0	0	1.62	1.61
0.875	5%	0	1.20	11.5	14.3	0	0	1.90	1.89
1.540	10%	0	2.00	11.0	6.18	0	0	1.17	1.15
0.985	10%	0	1.40	11.4	11.1	0	0	1.67	1.65
0.875	10%	0	1.20	11.5	14.3	0	0	1.96	1.94
1.540	0	1	2.00	11.0	6.18	0.297	0.445	1.10	1.10
0.985	0	1	1.40	11.4	11.1	0.133	0.200	1.57	1.57
0.875	0	1	1.20	11.5	14.3	0.0967	0.145	1.84	1.84
1.540	0	5	2.00	11.0	6.18	1.48	2.22	1.11	1.11
0.985	0	5	1.40	11.4	11.1	0.667	1.00	1.59	1.58
0.875	0	5	1.20	11.5	14.3	0.483	0.724	1.86	1.85

TABLE I. **Parameters of a deformed NS for AP4 EoS.** ρ_c is the central energy density, Ω/Ω_K is the angular velocity normalized by the mass-shedding limit $\Omega_K = \sqrt{M/R^3}$, \bar{Q} is the dimensionless quadrupole moment, M and R are the stellar mass and radius, \bar{I} is the normalized moment of inertia, $\bar{Q}\sigma_2/\sigma_0$ is the amplitude of the shell's surface density due to the quadrupole moment \bar{Q} normalized by a typical surface density, $\sigma_0 \approx 10^{18}$ g cm $^{-2}$, corresponding to 1% of the stellar mass, $(\Delta\gamma/\gamma_0)^{\text{equator}}$ is the anisotropy of the shell at the equator normalized by the pressure of the spherical shell, and ν_ϕ^{ISCO} and ν_θ^{ISCO} are the azimuthal frequency and the vertical epicyclic frequency at the innermost stable circular orbit (ISCO), see Sec. III.

ranges of compactness ($0.1 \lesssim M/R \lesssim 0.2$), whereas more massive and compact ($M/R \gtrsim 0.16$) oblate stars require smaller quadrupoles to maintain positive density at the poles.

More generically, it is noteworthy to study all the energy conditions for the thin-shell fluid. The null energy condition reads $\sigma + \gamma_i \geq 0$ (here $i = \theta, \phi$), the weak energy condition additionally requires $\sigma \geq 0$; in addition to the latter condition, the strong energy condition also requires $\sigma + \sum_i \gamma_i \geq 0$. Finally, the dominant energy condition requires only $\sigma > |\gamma_i|$. A detailed numerical exploration of the parameter space shows that all energy conditions are satisfied for any realistic ranges of compactness whenever $\bar{Q} \lesssim M_{\text{crust}}/M$. For the adopted reference value $M_{\text{crust}}/M \sim 0.01$, the condition $|\bar{Q}| \lesssim 0.01$ ensures that all energy conditions are satisfied for any compactness, whereas if $|\bar{Q}| \lesssim 0.1$ all energy conditions are satisfied for NSs with compactness $M/R \lesssim 0.15$.

C. Linear stability analysis

Performing a linear-stability analysis of deformed NSs is a challenging task, owing to the lack of symmetry of the background equilibrium solutions. To deal with this problem, we adopted a multi-parameter perturbative scheme, extending the techniques recently developed to study perturbations of slowly-rotating compact objects [42–44]. The computation can be summarized in the following steps [42]: (i) consider a complete set of small perturbations to the metric and the fluid variables, expanded in a basis of spherical harmonics $Y_{\ell m}(\theta, \phi)$; (ii) solve for the dynamical equations perturbatively to

leading order in the perturbation and to any given order in the background deformation; (iii) Fourier-transform the perturbation functions and reduce the dynamical equations to a system of ordinary (radial) differential equations; (iv) finally, solve for the system as an eigenvalue problem and obtain the characteristic modes of vibration. The eigenfrequencies ω are generically complex numbers and the sign of the imaginary part allows us to discriminate between stable and unstable configurations, owing to the $e^{-i\omega t}$ time dependence of the perturbations.

This standard procedure is made more involved by the broken symmetry of the background and by the presence of a thin shell. In an axially symmetric background, perturbations with different values of the azimuthal number m are still decoupled, but the intrinsic quadrupole deformation introduces mixing between modes with opposite parity and different multipolar indices.

For heuristic purposes, let us first consider the dynamics of a test scalar field ψ on the geometry of a deformed NS. By expanding $\psi = \sum_{\ell m} R_{\ell m}(r)r^{-1}Y_{\ell m}(\theta, \phi)e^{-i\omega t}$, the Klein-Gordon equation, $\square\psi = 0$, reduces to

$$\sum_{l=0}^{\infty} (A_\ell(r)Y_{\ell m} + D_\ell(r)P_2(\cos\theta)Y_{\ell m}(\theta, \phi)) = 0, \quad (28)$$

where A_ℓ and D_ℓ are complicated functions of $R_{\ell m}(r)$ and of its derivatives up to second order, and they also depend on the frequency ω and on the multipolar index ℓ . The function A_ℓ contains only quantities at zeroth order in the deformation, whereas the function D_ℓ is proportional to the quadrupolar deformation. Using the properties of the spherical harmonics [42], the above equation can be written as a system involving couplings between modes

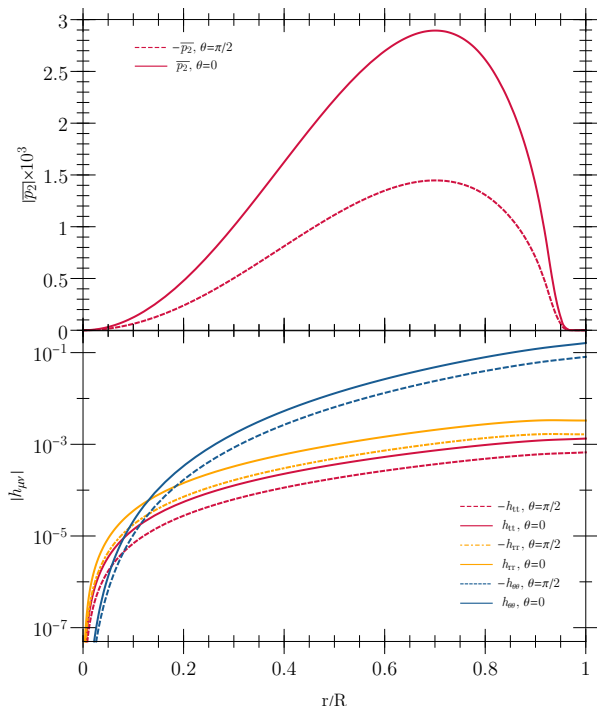


FIG. 3. **Internal solutions.** Radial profiles of the fluid and metric variables in the interior of a deformed NS evaluated along the equatorial direction ($\theta = \pi/2$, dashed lines) and polar direction ($\theta = 0$, solid lines). We show the profile of the pressure deformation (top panel) due to an intrinsic quadrupole deformation normalized by the central pressure of the object, $\bar{p}_2 \equiv (P(r, \theta) - P_0(r))/P_0(0)$, and the metric deformation functions $h_{\mu\nu} \equiv g_{\mu\nu} - g_{\mu\nu}^{(0)}$ (bottom panel). The solution corresponds to a nonspinning prolate object with $M = 1.4M_\odot$ and $\bar{Q} = 0.1$ to linear order in the deformation. To this order the deformations describing a nonrotating oblate object with the same magnitude of quadrupole ($\bar{Q} = -0.1$) are identical to those shown in this plot but with the opposite sign.

with harmonic index ℓ and $\ell \pm 2$:

$$\frac{2}{3}A_\ell + \left(C_{\ell+1}^2 + C_\ell^2 - \frac{1}{3}\right)D_\ell + C_\ell C_{\ell-1}D_{\ell-2} + C_{\ell+1}C_{\ell+2}D_{\ell+2} = 0, \quad (29)$$

where $C_\ell \equiv \sqrt{\frac{\ell^2 - m^2}{4\ell^2 - 1}}$. Formally, the above equation forms an infinite cascade of coupled ordinary differential equations since each ℓ mode is coupled to $\ell \pm 2$. However, assuming only ℓ -led perturbations to the leading order, the coupling to $\ell \pm 2$ modes is subleading (because $D_{\ell \pm 2} = \mathcal{O}(\bar{Q}^2)$) and Eq. (29) reduces to

$$A_\ell + \frac{3}{2} \left(C_{\ell+1}^2 + C_\ell^2 - \frac{1}{3}\right) D_\ell = 0, \quad (30)$$

which is now a single differential equation for the variable $R_{\ell m}$ (for each ℓ).

Remarkably, for radial perturbations ($\ell = m = 0$) the second term in Eq. (30) vanishes identically and

therefore radial perturbations are described by an equation of the form $A_0 = 0$, which coincides with the spherically-symmetric case. For $\ell > 0$, this property is lost and the second term in Eq. (30) yields some corrections. In this case the perturbation equation can be reduced to a Schrödinger-like equation of the form $d^2 R_{\ell m}/dx^2 + (\omega^2 - V_{\ell m})R_{\ell m} = 0$, where x is a new coordinates and the effective potential acquires a correction proportional to Q . In the exterior, the form of the potential can be computed analytically. An analysis of the potential and corresponding eigenvalue problem shows that there are no unstable modes for any ℓ .

Let us now turn to the more interesting case of gravitational perturbations. This is much more involved due to the tensorial nature of the perturbations and the coupling to the fluid modes. Nonetheless, in the radial case we can still obtain a system of equations which is formally equivalent to Eq. (30), where now A_ℓ and D_ℓ are vector functions of all metric and fluid perturbations. Thus, we obtain the remarkable result that, to linear order in the quadrupolar deformation, radial perturbations of a deformed NS are governed by the same equations as in the spherical case. In particular, this implies that deformed NSs are stable under radial perturbations for configurations below the maximum mass [6]. The case of axial dipolar ($\ell = 1$) perturbations and of axial and polar perturbations with $\ell \geq 2$ is much more involved, due to the coupling among different sectors, and is left for future work.

We note that, within our perturbative framework, the characteristic frequencies acquire small corrections proportional to Q . Therefore, only marginally stable modes in the spherical case can turn unstable. Instabilities, if they exist, can only come from the fluid axial sector for $\ell \geq 2$, which contains a zero mode ($\omega = 0$) in the spherical case. This mode can turn unstable due to the term proportional to Q , similarly to the case of the r-mode instability of slowly-spinning NSs [45–47], for which the unstable mode has $\omega = m\Omega$. If present, an r-mode-like instability might remove part of the intrinsic quadrupole moment until the mode is saturated.

III. PHENOMENOLOGICAL IMPLICATIONS

As previously shown, a thin crust with reasonable values of anisotropy can sustain an intrinsic (dimensionless) quadrupole moment as high as $\bar{Q} = \mathcal{O}(0.1)$, with more conservative values being $\bar{Q} = \mathcal{O}(0.01)$. The magnitude of the intrinsic quadrupole should be compared with the spin-induced quadrupole moment of a slowly-spinning NS, which scales quadratically with the dimensionless spin parameter, $\bar{Q}_{\text{spin}} = -\gamma\chi^2$, where $\gamma \approx 4 \div 7$ for compact stars with $M \approx 1.4M_\odot$, the precise number depending on the EoS [24, 25, 48, 49]. Since the spin χ of a NS is typically small [50] (roughly $\chi \approx 0.1$ for the fastest millisecond pulsars and likely much smaller for old NSs in coalescing binaries detectable by LIGO/Virgo), the spin-

induced quadrupole moment is at most $|\bar{Q}_{\text{spin}}| \approx 7 \times 10^{-2}$ and typically smaller. This suggests that any putative quadrupole moment of an old NS might predominantly natal rather than spin-induced. If this is the case, a deformed NS might provide a better model for the external spacetime of the body.

Any quantity X of a spinning, deformed NS contains independent J -induced and Q -induced corrections; schematically, up to second order in the deformation [31],

$$X = X_0 + X_{10}\chi + X_{01}\bar{Q} + X_{20}\chi^2 + X_{02}\bar{Q}^2 + X_{11}\chi\bar{Q}, \quad (31)$$

where X_0 is the value of the corresponding spherically-symmetric star and X_{ij} are corrections that only depend on the EoS and on the central density of the star. When $Q = 0$, we recover the well-known case of a slowly-spinning NS [24, 25].

A. Corrections of geodesic frequencies due to an intrinsic quadrupole

The external metric can be used to study how the spacetime of a deformed NS is affected by its intrinsic quadrupole. All geodesic quantities – including the ISCO and the epicyclic frequencies – acquire corrections as in Eq. (31), which affect properties such as the innermost location of an accretion disk and, in turn, the corresponding electromagnetic flux from accreting low-mass X-ray binaries, whose signal originates very deep in the gravitational field of the accreting object, at distances down to a few gravitational radii [51]. To linear order, the azimuthal frequency (ν_ϕ) and the vertical epicyclic frequency (ν_θ) at the ISCO read (see Appendix A)

$$\nu_\phi^{\text{ISCO}} \approx 1.57 (1 + 0.75\chi + 0.23\bar{Q}) \left(\frac{1.4M_\odot}{M} \right) \text{ kHz} \quad (32)$$

$$\nu_\theta^{\text{ISCO}} \approx 1.57 (1 + 0.61\chi + 0.17\bar{Q}) \left(\frac{1.4M_\odot}{M} \right) \text{ kHz} \quad (33)$$

independently of the NS EoS. When $\bar{Q} \approx 0.1$, these frequencies can differ by a few percent relative to the spherical case, leading to deviations in the emitted flux of the same order. The quadrupolar correction is larger than the spin-induced linear term whenever $\bar{Q} \gtrsim 0.18 \left(\frac{\chi}{0.05} \right)$.

B. GW phase corrections due to an intrinsic quadrupole

NSs in compact binaries are assumed to be spherically symmetric at large orbital distance d , whereas they are deformed during the coalescence due to tidal interactions [54]. The tidally-induced quadrupole moment is proportional to the tidal field $\sim M/d^3$; the leading-order tidal correction to the GW phase enters at the fifth post-

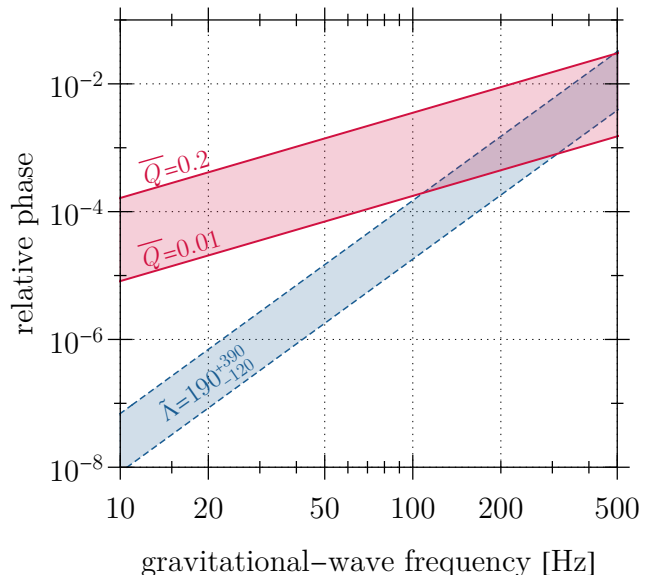


FIG. 4. **GW phase.** Phase contribution, $\phi_{\text{quadrupole}}$, for the coalescence of two NSs with intrinsic quadrupole moment relative to the leading-order Newtonian term in the LIGO band. The red band corresponds to the range $\bar{Q} \in (0.01, 0.2)$. The effect of the intrinsic deformation is larger than that of the tidal deformability (blue band) below $100 \div 200$ Hz even for (normalized) intrinsic quadrupole moment as small $\bar{Q} \approx 0.01$, and it always dominates at lower frequencies or for higher deformations. We use reference values $m_1 = m_2 = 1.4M_\odot$, and tidal deformability $\tilde{\Lambda} = 190_{-120}^{+390}$ [52, 53].

Newtonian² order [55], i.e. $\phi_{\text{tidal}} \sim v^5$, and it is proportional to the tidal deformability $\tilde{\Lambda}$, which characterizes the size of the tidally induced quadrupole deformations of the two stars [10, 54].

On the other hand, an intrinsic quadrupole moment of the two inspiraling bodies affects the GW phase already at second post-Newtonian order [55, 56]. Adapting the results for a spin-induced quadrupole moment, we find that a generic quadrupole moment gives the following GW phase contribution

$$\phi_{\text{quadrupole}} = \frac{75}{64} \frac{(m_1^2 \bar{Q}_1 + m_2^2 \bar{Q}_2)}{m_1 m_2} \frac{1}{v} \simeq \frac{75}{32} \frac{\bar{Q}}{v}, \quad (34)$$

where in the last step we assumed the same masses ($m_1 = m_2 = M$) and the same intrinsic quadrupole moment ($\bar{Q}_1 = \bar{Q}_2 = \bar{Q}$) for the two stars. As long as $\bar{Q} \approx 0.01$ or larger, the effect of the intrinsic quadrupole will dominate over the tidal term, especially at low frequencies (Fig. 4). To the best of our knowledge, this

² The post-Newtonian approach is a weak-field/slow-velocity expansion of Einstein's equations, where the expansion parameter is the orbital velocity $v \ll 1$. A n -th post-Newtonian correction to the GW phase corresponds to a term that is suppressed by v^{2n} relative to the leading-order, $\sim v^{-5}$, contribution.

effect has never been considered before, but can dramatically affect the parameter estimation of NS binaries and significantly modify the constraints on the NS EoS [10, 52, 53].

IV. DISCUSSION

Although our analysis is based on some simplified assumptions, it suggests that intrinsic deformations in NSs could have important implications for high-energy astrophysics, GW astronomy, and nuclear physics. Deformed NSs might provide a more accurate description for the interior of NSs in binary systems and, in turn, for all the strong-gravity phenomena which are analyzed to infer the NS EoS.

It is difficult to estimate the degree of deformation expected for NSs formed in realistic situations, e.g. in a merger, since the latter is often simulated with simplified initial data, with some assumed degree of symmetry, and the evolution is typically stopped before the remnant has reached a truly stationary configuration. More importantly, numerical simulations typically use perfect fluids, which cannot sustain deformations away from spherical symmetry in the static case [33]. Although the (micro)physics of a NS interior is very complex [29, 34, 35], deformations might be the rule rather than the exception [30]. Indeed, relatively large quadrupole moments can be sustained even by modest anisotropic stresses, as we showed. Another example is the case of self-gravitating elastic compact objects. In general, even in the static case, these objects do not need to be spherical since deformations from spherical symmetry can be supported by shears in the material [57, 58]. A very interesting extension of our work is to construct deformed NSs sustained by elasticity beyond the thin-shell formalism adopted here.

We have explicitly focused on the case of an anisotropic crust, but nonspherical deformations might also be sourced by other processes, for example by a magnetic field. Relativistic models of axisymmetric, highly-magnetized NSs have been studied in great detail, see e.g. [18–23]. The quadrupole moment induced by the magnetic field B can be parametrized as

$$\bar{Q} = -\beta \frac{\pi B^2 R^8}{\mu_0 I M^3} \approx -0.01 \beta \frac{B_{16}^2 R_{12}^8}{I_{45} M_{1.4}^3}, \quad (35)$$

where $B_{16} = \frac{B}{10^{16} \text{ Gauss}}$, $R_{12} = \frac{R}{12 \text{ km}}$, $M_{1.4} = \frac{M}{1.4 M_\odot}$, $I_{45} = \frac{I}{10^{45} \text{ g cm}^2}$, I is the moment of inertia, μ_0 is the vacuum permeability, and $\beta \sim \mathcal{O}(1)$ is the magnetic distortion factor which measures to what extent a star can be deformed by the magnetic field. Note the very strong dependence on the radius of the star R and the quadratic dependence on the magnetic field B . By computing M , R , and I for a family of NSs with some tabulated EoS, one can check that the magnetic-induced \bar{Q} is of the order of what given in Eq. (35) for all configurations, and

therefore very small unless the magnetic field is extreme. In the case of deformation sourced by a magnetic field, the exterior of the star is not vacuum, so strictly speaking our solution in the exterior is not valid. However, the magnetic field is mainly dipolar and decays as r^{-3} . Sufficiently far from the star, the vacuum solution is a good approximation and the metric can be matched to the analytical one written in terms of the multipole moments [31].

Observational bounds on parametrized corrections to the post-Newtonian coefficient at second order from binary-NS coalescence GW170817 ($\delta\varphi_2 \lesssim 3.5$ at 90% confidence level [59]) can be directly translated – using Eq. 34 – into a bound on the intrinsic quadrupole moments of the binary components, yielding $Q \lesssim 0.14$ (assuming equal masses). This justifies our perturbative treatment but does not exclude that the binary components of GW170817 had some significant intrinsic deformation. This also suggests that a putative measurement $\delta\varphi_2 \neq 0$ in the future might be due to an intrinsic deformation of the NSs rather than to a fundamental departure from general relativity.

An outstanding issue concerns the stability of deformed NSs at equilibrium. Performing a linear stability analysis is particularly challenging due to the broken symmetry of the equilibrium configuration. Nevertheless, such an analysis can be performed using advanced perturbation-theory techniques developed for slowly-spinning compact objects [42–44]. A preliminary analysis shows that deformed NSs are stable against radial perturbations for masses below the maximum mass, exactly as spherically-symmetric NSs [6] and other thin-shell objects like gravastars [41]. Within our perturbative framework, possible instabilities might only come from (axial) nonaxisymmetric fluid perturbations, which are the only ones containing a *zero mode* in the spherical case. This mode can turn unstable due to the correction proportional to Q , similarly to the case of the r-mode instability of slowly-spinning NSs [45–47]. If present, an r-mode-like instability might remove part of the intrinsic quadrupole moment until the mode is saturated by GW emission or other mechanisms.

To second order in the deformations, the coupling between J and Q moments induces novel multipole moments through the standard angular-momentum addition rules [31]. In particular, it induces a mass hexadecapole and a current octupole, as well as a shift of the stellar mass and radius, angular momentum, and mass quadrupole moment. These corrections are quadratic in the deformation and therefore subleading. For example, for $\bar{Q} \approx 0.1$ in the nonspinning case the NS mass acquires a correction approximately at the percent level, which is comparable to the mass of the crust [29]. On the other hand, higher-order corrections might be important to model highly-deformed stars more accurately.

To summarize, using a simple thin-shell model, we showed that anisotropic crust stresses can support significant quadrupolar deformations while satisfying all en-

ergy conditions. Based on this model, we argue that if NSs display some departure from spherical symmetry of the order of at least a few tenths of a percent, their intrinsic quadrupole moment would introduce corrections that are more important than the spin and tidal deformations. We advocate the urgency of quantifying NS intrinsic deformations and of including them in the parameter estimation of electromagnetic and GW signals from isolated and binary NSs.

ACKNOWLEDGMENTS

We are indebted with Carlos Palenzuela for initial collaboration that lead to this work. We are also grateful to Vitor Cardoso, Valeria Ferrari, Bruno Giacomazzo, Kostas Kokkotas, Massimo Mannarelli, and Luigi Stella for interesting discussion. P.P. acknowledges financial support provided under the European Union's H2020 ERC, Starting Grant agreement no. DarkGRA-757480, and under the MIUR PRIN and FARE programmes (GW-NEXT, CUP: B84I20000100001). The authors would like to acknowledge networking support by the COST Action CA16104 and support from the Amaldi Research Center funded by the MIUR program "Dipartimento di Eccellenza" (CUP: B81I18001170001).

Appendix A: Epicyclic frequencies

The epicyclic frequencies can be computed for a generic stationary, axisymmetric spacetime [60]. Setting the spin to zero, to the leading order in \bar{Q} , the azimuthal frequency and the vertical and radial epicyclic frequencies read

$$\nu_\phi = \frac{1}{2\pi M x^{3/2}} (1 + \Delta_\phi \bar{Q}) , \quad (\text{A1})$$

$$\nu_\theta = \frac{1}{2\pi M x^{3/2}} (1 + \Delta_\theta \bar{Q}) , \quad (\text{A2})$$

$$\nu_r = \frac{\sqrt{x-6}}{2\pi M x^2} (1 + \Delta_r \bar{Q}) , \quad (\text{A3})$$

respectively, where $x \equiv r/M$ and

$$\Delta_\phi = \frac{-15(x-2)x(x^3-2)\log\left(\frac{x-2}{x}\right) + 10x(x(2-3(x-1)x)+8) - 60}{32(x-2)x} ,$$

$$\Delta_\theta = \frac{5}{32} \left(6x(2x-7) - \frac{12}{(x-2)x} + 3(2x-1)(x-2)^2 \log\left(\frac{x-2}{x}\right) + 34 \right) ,$$

$$\Delta_r = \frac{10(48 + x(30 + x(26 + x(3(25 - 4x)x - 127)))) - 15(x-2)^2 x^2 (x(4x-13) - 2) \log\left(\frac{x-2}{x}\right)}{32(x-6)(x-2)x} .$$

For completeness, we also provide the leading-order quadrupolar corrections to the ISCO radius in closed form, including also the well-known spin term at the linear order:

$$r_{\text{ISCO}} = 6M \left[1 - \frac{2\sqrt{2}}{3\sqrt{3}}\chi + \left(\frac{9325}{96} - 480 \coth^{-1}(5) \right) \bar{Q} \right] , \quad (\text{A4})$$

and the corresponding analytical expressions for ν_ϕ and ν_θ at the ISCO:

$$\nu_\phi^{\text{ISCO}} = \frac{1}{12\pi\sqrt{6}M} \left[1 + \frac{11}{6\sqrt{6}}\chi + \frac{5}{32} (5892 \coth^{-1}(5) - 1193) \bar{Q} \right] , \quad (\text{A5})$$

$$\nu_\theta^{\text{ISCO}} = \frac{1}{12\pi\sqrt{6}M} \left[1 + \frac{\sqrt{3}}{2\sqrt{2}}\chi + \left(555 \coth^{-1}(5) - \frac{3595}{32} \right) \bar{Q} \right] . \quad (\text{A6})$$

An approximate version of the above equations has been presented in the main text.

[1] J. M. Lattimer and M. Prakash, *Science* **304**, 536 (2004), arXiv:astro-ph/0405262 [astro-ph].

[2] B. Carter, *Phys. Rev. Lett.* **26**, 331 (1971).

- [3] S. Hawking and G. Ellis, *The Large scale structure of space-time* (1973).
- [4] R. P. Geroch, *J.Math.Phys.* **11**, 2580 (1970).
- [5] R. Hansen, *J.Math.Phys.* **15**, 46 (1974).
- [6] S. L. Shapiro and S. A. Teukolsky, *Black holes, white dwarfs, and neutron stars: The physics of compact objects* (Wiley, 1983).
- [7] S. A. Colgate and R. H. White, *ApJ* **143**, 626 (1966).
- [8] H.-T. Janka, K. Langanke, A. Marek, G. Martinez-Pinedo, and B. Mueller, *Phys. Rept.* **442**, 38 (2007), arXiv:astro-ph/0612072 [astro-ph].
- [9] M. Shibata, K. Taniguchi, and K. Uryu, *Phys. Rev. D* **71**, 084021 (2005), arXiv:gr-qc/0503119 [gr-qc].
- [10] B. P. Abbott, R. Abbott, T. D. Abbott, F. Acernese, K. Ackley, C. Adams, T. Adams, P. Addesso, R. X. Adhikari, V. B. Adya, and et al., *Physical Review Letters* **119**, 161101 (2017), arXiv:1710.05832 [gr-qc].
- [11] L. Baiotti, B. Giacomazzo, and L. Rezzolla, *Phys. Rev. D* **78**, 084033 (2008), arXiv:0804.0594 [gr-qc].
- [12] N. Andersson, K. D. Kokkotas, and B. F. Schutz, *Astrophys. J.* **510**, 846 (1999), arXiv:astro-ph/9805225 [astro-ph].
- [13] K. Glampedakis and L. Gualtieri, “Gravitational waves from single neutron stars: an advanced detector era survey,” (2018) pp. 673–736, arXiv:1709.07049 [astro-ph.HE].
- [14] K. Glampedakis, D. I. Jones, and L. Samuelsson, *Phys. Rev. Lett.* **109**, 081103 (2012), arXiv:1204.3781 [astro-ph.SR].
- [15] G. Ushomirsky, C. Cutler, and L. Bildsten, *Mon. Not. Roy. Astron. Soc.* **319**, 902 (2000), arXiv:astro-ph/0001136 [astro-ph].
- [16] B. Haskell, D. I. Jones, and N. Andersson, *Mon. Not. Roy. Astron. Soc.* **373**, 1423 (2006), arXiv:astro-ph/0609438 [astro-ph].
- [17] B. P. Abbott *et al.* (LIGO Scientific, Virgo), *Astrophys. J.* **875**, 122 (2019), arXiv:1812.11656 [astro-ph.HE].
- [18] K. Ioka and M. Sasaki, *Astrophys. J.* **600**, 296 (2004), arXiv:astro-ph/0305352.
- [19] A. Colaiuda, V. Ferrari, L. Gualtieri, and J. A. Pons, *Mon. Not. Roy. Astron. Soc.* **385**, 2080 (2008), arXiv:0712.2162 [astro-ph].
- [20] J. Frieben and L. Rezzolla, *MNRAS* **427**, 3406 (2012), arXiv:1207.4035 [gr-qc].
- [21] A. G. Pili, N. Bucciantini, and L. Del Zanna, *MNRAS* **439**, 3541 (2014), arXiv:1401.4308 [astro-ph.HE].
- [22] N. Bucciantini, A. G. Pili, and L. Del Zanna, *MNRAS* **447**, 3278 (2015), arXiv:1412.5347 [astro-ph.HE].
- [23] M. Bocquet, S. Bonazzola, E. Gourgoulhon, and J. Novak, *A&A* **301**, 757 (1995), arXiv:gr-qc/9503044 [gr-qc].
- [24] J. B. Hartle, *Astrophys. J.* **150**, 1005 (1967).
- [25] J. B. Hartle and K. S. Thorne, *ApJ* **153**, 807 (1968).
- [26] K. Rajagopal and R. Sharma, *Physical Review D* **74** (2006), 10.1103/physrevd.74.094019.
- [27] K. Rajagopal and R. Sharma, *Journal of Physics G: Nuclear and Particle Physics* **32**, S483–S490 (2006).
- [28] M. G. Alford, A. Schmitt, K. Rajagopal, and T. Schäfer, *Reviews of Modern Physics* **80**, 1455–1515 (2008).
- [29] N. Chamel and P. Haensel, *Living Rev. Rel.* **11**, 10 (2008), arXiv:0812.3955 [astro-ph].
- [30] D. A. Baiko and A. I. Chugunov, *Mon. Not. Roy. Astron. Soc.* **480**, 5511 (2018), arXiv:1808.06415 [astro-ph.HE].
- [31] G. Raposo, P. Pani, and R. Emparan, *Phys. Rev. D* **99**, 104050 (2019), arXiv:1812.07615 [gr-qc].
- [32] T. Hinderer, *Astrophys. J.* **677**, 1216 (2008), Erratum: *ibid.* **697**, 964 (2009), arXiv:0711.2420 [astro-ph].
- [33] L. Lindblom and A. K. M. Masood-Ul-Alam, *Communications in Mathematical Physics* **162**, 123 (1994).
- [34] P. Haensel, A. Potekhin, and D. Yakovlev, *Neutron Stars 1: Equation of State and Structure* (Springer, 2007).
- [35] M. E. Caplan and C. J. Horowitz, *Rev. Mod. Phys.* **89**, 041002 (2017), arXiv:1606.03646 [astro-ph.HE].
- [36] W. Israel, *Nuovo Cim.* **B44S10**, 1 (1966), [Nuovo Cim.B44,1(1966)].
- [37] M. Visser, *Lorentzian wormholes: From Einstein to Hawking* (1995).
- [38] A. Maselli, P. Pani, L. Gualtieri, and V. Ferrari, *Phys. Rev. D* **92**, 083014 (2015), arXiv:1507.00680 [gr-qc].
- [39] Relevant codes to construct deformed NS solutions are publicly available at <https://web.uniroma1.it/gmunu>.
- [40] N. Uchikata and S. Yoshida, *Class. Quant. Grav.* **33**, 025005 (2016), arXiv:1506.06485 [gr-qc].
- [41] N. Uchikata, S. Yoshida, and P. Pani, *Phys. Rev. D* **94**, 064015 (2016), arXiv:1607.03593 [gr-qc].
- [42] P. Pani, *Proceedings, Spring School on Numerical Relativity and High Energy Physics (NR/HEP2): Lisbon, Portugal, March 11-14, 2013*, *Int. J. Mod. Phys. A* **28**, 1340018 (2013), arXiv:1305.6759 [gr-qc].
- [43] P. Pani, L. Gualtieri, A. Maselli, and V. Ferrari, *Phys. Rev. D* **92**, 024010 (2015), arXiv:1503.07365 [gr-qc].
- [44] P. Pani, L. Gualtieri, and V. Ferrari, *Phys. Rev. D* **92**, 124003 (2015), arXiv:1509.02171 [gr-qc].
- [45] N. Andersson, *Astrophys. J.* **502**, 708 (1998), arXiv:gr-qc/9706075 [gr-qc].
- [46] J. L. Friedman and S. M. Morsink, *Astrophys. J.* **502**, 714 (1998), arXiv:gr-qc/9706073 [gr-qc].
- [47] N. Andersson and K. D. Kokkotas, *Int. J. Mod. Phys. D* **10**, 381 (2001), arXiv:gr-qc/0010102 [gr-qc].
- [48] K. Yagi and N. Yunes, *Science* **341**, 365 (2013), arXiv:1302.4499 [gr-qc].
- [49] K. Yagi and N. Yunes, *Phys. Rept.* **681**, 1 (2017), arXiv:1608.02582 [gr-qc].
- [50] T. Dietrich, N. Moldenhauer, N. K. Johnson-McDaniel, S. Bernuzzi, C. M. Markakis, B. Bruggmann, and W. Tichy, *Phys. Rev. D* **92**, 124007 (2015), arXiv:1507.07100 [gr-qc].
- [51] M. van der Klis, *Ann. Rev. Astron. Astrophys.* **38**, 717 (2000), arXiv:astro-ph/0001167 [astro-ph].
- [52] B. P. Abbott *et al.* (LIGO Scientific, Virgo), *Phys. Rev. Lett.* **121**, 161101 (2018), arXiv:1805.11581 [gr-qc].
- [53] S. De, D. Finstad, J. M. Lattimer, D. A. Brown, E. Berger, and C. M. Biwer, *Phys. Rev. Lett.* **121**, 091102 (2018), [Erratum: *Phys. Rev. Lett.*121,no.25,259902(2018)], arXiv:1804.08583 [astro-ph.HE].
- [54] E. E. Flanagan and T. Hinderer, *Phys. Rev. D* **77**, 021502 (2008), arXiv:0709.1915 [astro-ph].
- [55] L. Blanchet, *Living Rev. Rel.* **9**, 4 (2006).
- [56] N. V. Krishnendu, K. G. Arun, and C. K. Mishra, *Phys. Rev. Lett.* **119**, 091101 (2017), arXiv:1701.06318 [gr-qc].
- [57] L. Andersson, R. Beig, and B. G. Schmidt, *Commun. Pure Appl. Math.* **61**, 988 (2008), arXiv:gr-qc/0611108 [gr-qc].
- [58] L. Andersson, R. Beig, and B. G. Schmidt, *Commun. Pure Appl. Math.* **63**, 559 (2009), arXiv:0811.0932 [gr-qc].
- [59] B. P. Abbott *et al.* (LIGO Scientific, Virgo), arXiv:1811.00364 (preprint) (2018).

[60] A. Maselli, L. Gualtieri, P. Pani, L. Stella, and V. Fer-

rari, *Astrophys. J.* **801**, 115 (2015), arXiv:1412.3473 [astro-ph.HE].